Interaction of LDS-751 and Rhodamine 123 with P-Glycoprotein: Evidence for Simultaneous Binding of Both Drugs[†]

Miguel R. Lugo[‡] and Frances J. Sharom*[,§]

Department of Molecular and Cellular Biology, University of Guelph, Guelph, Ontario, Canada N1G 2W1, and Instituto de Biología Experimental, Facultad de Ciencias, Universidad Central de Venezuela, Caracas, Venezuela

Received June 10, 2005; Revised Manuscript Received August 22, 2005

ABSTRACT: The P-glycoprotein efflux pump, an ABC superfamily member, can export a wide variety of hydrophobic drugs, natural products, and peptides from cells, powered by the energy of ATP hydrolysis. Transport substrates appear to first partition into the membrane and then interact with the protein within the cytoplasmic leaflet. Two drug binding sites within P-glycoprotein have been described which interact allosterically, the H-site (binds Hoechst 33342) and the R-site (binds rhodamine 123); however, the structural and functional relationship between the various binding sites appears complex. In this work, we have used fluorescence spectroscopic approaches to characterize the interaction of the transporter with LDS-751 and rhodamine 123, both of which are believed to bind to the putative R-site based on functional transport studies. By carrying out single and sequential dual fluorescence titrations of purified P-glycoprotein with the two substrates, we observed that bound LDS-751 interacted with bound rhodamine 123. Rhodamine 123 and LDS-751 showed a reciprocal negative interaction, each reducing the binding affinity of the other by 5-fold, indicating that the two compounds were simultaneously bound to the protein to form a ternary complex. Fitting of the dependence of the apparent K_d for LDS-751 binding on rhodamine 123 concentration suggested that the two compounds interacted noncompetitively. We conclude that the two-site drug binding model for P-glycoprotein requires modification. The putative R-site appears large enough to accommodate two compounds simultaneously. The locations where LDS-751 and rhodamine 123 bind are likely adjacent to each other, possibly overlapping, and may be within a hydrophobic pocket.

The P-glycoprotein multidrug transporter (Pgp)[1] is a polyspecific ATP-binding cassette (ABC) protein that pumps a wide variety of structurally unrelated substrates across the membrane in an ATP-dependent manner, causing the multidrug-resistant (MDR) phenotype (*1*−*3*). Among the compounds it transports are anthracyclines, *Vinca* alkaloids, taxanes, cytotoxic agents, linear and cyclic peptides, ionophores, steroids, fluorescent dyes, and detergents (*4*). Similarly, a large number of structurally unrelated compounds, known as modulators, are able to reverse Pgp-mediated MDR, by either competing with transport substrates for interaction with the drug binding sites or by acting allosterically. This suggests the possibility of multiple or overlapping substrate/modulator-binding domains on the transporter, leading to much speculation concerning the number, nature, location, and relationships of the binding site(s) (for example, see ref *5*).

Diverse experimental approaches have been used to address the problem, each of them with their own technical difficulties, advantages, and disadvantages. Several groups reported the influence of drugs and modulators on Pgp ATPase activity (*6*−*8*). The goal of this approach was to describe the interaction of each drug with Pgp in terms of (i) the number of binding sites, (ii) the affinity of binding, (iii) the effector factor (the influence on the rate of ATP hydrolysis), and (iv) the interaction factor between drugs (the change in substrate affinity). A puzzling observation is that not all substrates stimulate ATPase activity; several transported substrates actually inhibit activity in a concentration-dependent manner. Moreover, ATPase profiles are often biphasic, with stimulation at low drug concentrations, and inhibition at higher concentrations, while some classical MDR drugs such colchicine and doxorubicin barely affect Pgp ATPase activity. Borgnia et al. (*9*) assumed that stimulators and inhibitors both compete in classical Michaelis−Menten fashion with an endogenous substrate for a common site, while Orlowski and co-workers (*10*) concluded that Pgp possesses multiple binding sites with nonexclusive interactions. Similarly, Wang et al. (*11*) used a kinetic approach to show the presence of at least two substrate binding sites, which displayed noncompetitive or mixed-type inhibition.

Drug transport studies in whole cells and membrane vesicle systems (either native or reconstituted) have also addressed the issue of multiple drug binding sites. However, an inherent problem with transport experiments arises from

[†] This work was supported by a grant to F.J.S. from the Canadian Cancer Society and by the Council of Scientific and Humanistic Development of Venezuela (CDCH-UCV).

* To whom correspondence should be addressed. Phone: (519) 824-4120 ext 52247. Fax: (519) 837-1802. E-mail: fsharom@uoguelph.ca.

[‡] Universidad Central de Venezuela.

[§] University of Guelph.

[1] Abbreviations: ABC, ATP-binding cassette; CHAPS, 3-[(3-cholamidopropyl)dimethylammonio]-1-propanesulfonate; DMSO, dimethyl sulfoxide; H33342, Hoechst 33342; FRET, fluorescence resonance energy transfer; LDS-751, 2-[4-(4-[dimethylamino]phenyl)-1,3-butadienyl]-3-ethylbenzothiazolium perchlorate; MDR, multidrug resistant/resistance; NB, nucleotide binding; R123, rhodamine 123; TM, transmembrane; TMEA, tris(2-maleimidoethyl)amine.

10.1021/bi0511179 CCC: $30.25
Published on Web 09/30/2005

the relatively high rate of passive diffusion of hydrophobic substrates across the membrane. As a result, the observed rate of drug transport represents a balance between two opposing processes: active pumping by Pgp up a concentration gradient and passive diffusion of drug across the membrane down a concentration gradient. Several early reports mistakenly applied Michaelis−Menten analysis to equilibrium transport data. To overcome this problem, Sharom and co-workers employed the median effect to analyze drug transport in plasma membrane vesicles (*12*). Although this method is useful for analysis and quantitative comparison of equilibrium drug uptake data, it does not reflect the underlying molecular interaction (indeed, it is mechanism-independent) and does not give binding or kinetic constants. The classical Michaelis−Menten scheme was employed by Stein's group (*13*, *14*), who creatively manipulated the expression describing the process and obtained, with a minimum of assumptions, a model-dependent working equation which successfully described the competitive, noncompetitive, and cooperative interactions between several Pgp modulators. Real-time measurements of multidrug transport in intact cells (for example, see refs *15*, *16*) found noncompetitive inhibition between some substrates and Hill numbers >1 for others. Methods to determine transport rates involving continuous monitoring of fluorescent dyes employed native plasma membrane vesicles (*17*−*20*), or reconstituted Pgp in proteoliposomes (*21*, *22*), to provide insight into the number of sites and the relationship between them.

Photoaffinity labeling has emerged as a powerful technique to study the ligand-binding properties of Pgp. Competition experiments with photoactive substrate analogues have illustrated interactions between substrates and modulators, and indicated the presence of more than one drug binding site. Particularly, experiments combining enzymatic digestion and immunoprecipitation have mapped labeling to two sites within the N- and C-halves of Pgp, compatible with the idea of either two different binding sites, one in each half of the protein, or one binding site formed from the two homologous halves (*23*). More recently, three binding sites have been reported (*24*). However, photoactive drugs might label an interior site in Pgp that is not involved in the initial binding, and there is no evidence that the labeling site is coincident with the drug-binding site (*25*). In addition, most photoaffinity labeling studies suffer from the drawback of low labeling stoichiometry, so that often only a very small fraction of the total protein molecules are labeled. A recent photolabeling study used homology modeling to localize the labeling sites to the interfaces between the two transmembrane (TM) halves of Pgp (*26*). Several peptide fragments were covalently labeled with two ligands, which suggested that simultaneous binding of two substrate molecules is possible.

Despite technical limitations, radioligand-binding assays are the most direct probe of protein−ligand interactions. Tamai and Safa first used this approach to demonstrate the existence within Pgp of different substrate binding sites that interacted noncompetitively (*27*). Since then, binding and kinetic measurements with radioligands have shown the existence of multiple binding sites on Pgp that are allosterically linked (*28*−*30*).

Fluorescence spectroscopic techniques can be used to study Pgp−drug interactions in a direct manner. In this regard, our laboratory has developed various fluorescence quenching approaches to quantitate the binding of drugs to purified Pgp, either using an extrinsic fluorophore covalently linked to Pgp (*31*) or using native Trp fluorescence (*32*). K_d values for a large number of drugs and modulators from many different structural classes have been reported (*33*, *34*), which are in agreement with the relative affinities of these compound as assessed by other methods. Indeed, the K_d for binding to Pgp is highly correlated, over more than 3 orders of magnitude, with the IC_{50} for inhibition of drug transport for a large number of compounds (*33*, *34*). Fluorescence-based approaches have provided some evidence for simultaneous binding of two compounds to Pgp; for example, peptides showed monophasic Trp quenching curves while other non-peptide drugs presented biphasic curves (*32*).

It is, perhaps, not surprising that the literature presents varied and even contradictory results with respect to the number of Pgp drug and modulator binding sites, and their inter-relationships. Nevertheless, the transporter is proposed to contain two "operational" drug transport sites, referred to as the H-site and the R-site, for their preference for Hoechst 33342 (H33342) and rhodamine 123 (R123), respectively (*18*). These sites essentially present a phenomenological description, based on an increased or decreased rate of transport of one drug in the presence of another. A previous report indicated that the dye 2-[4-(4-[dimethylamino]phenyl)-1,3-butadienyl]-3-ethylbenzothiazolium perchlorate (LDS-751) interacts preferentially with the R-site (*19*), and the location of this site within Pgp was recently mapped using fluorescence resonance energy transfer (FRET) studies (*35*). The present work uses a fluorescence approach to provide additional experimental evidence about the nature of the R-site with respect to its selectivity toward various substrates. Results show that the putative R-site is large enough to accommodate two drugs, LDS-751 and R123, simultaneously, where they affect each other's binding in a noncompetitive manner.

EXPERIMENTAL PROCEDURES

Materials. 3-[(3-Cholamidopropyl)dimethylammonio]-1-propanesulfonate (CHAPS) and R123 were purchased from Sigma Chemical Co. (St. Louis, MO). LDS-751 was obtained from Molecular Probes (Eugene, OR).

Plasma Membrane Preparation and Pgp Purification. Plasma membrane vesicles were isolated from MDR CH^R-B30 Chinese hamster ovary cells (*36*) and stored at −70 °C for no more than 3 months before use. Pgp was isolated from plasma membrane vesicles using a two-step selective extraction with CHAPS. After treatment of the membrane vesicles with 25 mM CHAPS in Tris buffer (50 mM Tris-HCl/0.15 M NaCl/5 mM $MgCl_2$, pH 7.5) and centrifugation, the resulting S_1 pellet was solubilized in 15 mM CHAPS/Tris buffer as described previously (*31*). Affinity chromatography on Concanavalin-A-Sepharose was used to further purify Pgp from the soluble S_2 fraction. The final preparation consisted of 90−95% pure Pgp in 2 mM CHAPS/Tris buffer. Protein was quantitated by the method of Peterson (*37*) for purified Pgp, and by the method of Bradford (*38*) for plasma membrane, using bovine serum albumin (crystallized and lyophilized, Sigma) as a standard.

Fluorescence Measurements. Fluorescence spectra were recorded on a PTI Alphascan-2 spectrofluorimeter (Photon Technology International, London, ON, Canada) with the

cell holder thermostated at the indicated temperature. Stock solutions of LDS-751 and R123 were prepared in dimethyl sulfoxide (DMSO) at 5 mM and 1 mM, respectively (1000-fold higher than the highest desired final concentration); both were stored at −20 °C. Working solutions were prepared fresh in 2 mM CHAPS/Tris buffer, kept protected from the light and used within 3 h. Fluorescence emission spectra were recorded using a built-in automatic correction system.

Single titration experiments were performed by successively adding 5 μL aliquots of the working solution of LDS-751 to either 500 μL of 2 mM CHAPS/Tris buffer (control experiment) or 470 μL of Pgp (100 μg/mL) in 2 mM CHAPS/Tris buffer preincubated with R123 (from 0 to 30 μL of the working solution) in a quartz cell with a path length of 0.5 cm. The total volume of the ligand added during the titration was always 60 μL (13 titration points), which was 12% of the initial volume. The excitation wavelength was set at 550 nm and emission at 660 nm (both with 4 nm bandwidth). The measured fluorescence intensity was corrected for light scattering and the inner filter effect at both excitation and emission wavelengths as described elsewhere (*39*, *40*), using the expression

$$F_i^{cor} = (F_i - F_b) \times 10^{0.5(A_{\lambda ex} + A_{\lambda em})_i} \quad (1)$$

where F_i^{cor} is the corrected value of the fluorescence intensity, F_i is the experimental measured fluorescence intensity, F_b is the background fluorescence intensity caused by scattering (2 mM CHAPS/Tris buffer), and $A_{\lambda ex}$ and $A_{\lambda em}$ are the absorbance of the sample at the excitation and emission wavelengths for point *i* of the titration, respectively. In the presence of Pgp, F_b is the background fluorescence intensity caused by 0.1 mg/mL Pgp in 2 mM CHAPS/Tris buffer, and the dilution of the probe (bound LDS-751) was corrected according to

$$F_i^{cor} = (F_i - F_b)\frac{V_i}{V_0} \times 10^{0.5(A_{\lambda ex} + A_{\lambda em})_i} \quad (2)$$

where V_0 is the initial volume of the sample and V_i is the volume at a given point in the titration.

Double titration experiments were performed in essentially the same way as single ones. The difference in this protocol arises from the fact that, after titration with the first substrate (six points plus one background), the solution was titrated with the second substrate (six additional points). Double titrations were performed in both of the two possible sequences, changing the order of the half-titrations: (i) first with R123, then with LDS-751, and (ii) first with LDS-751, then with R123; in both cases the same final concentration of each substrate was attained. Equation 2 was used to correct for the inner filter effect and dilution of the bound dyes (or the protein). In addition, the final total concentration of the first substrate after the first half-titration was corrected for dilution at each point of the second half-titration.

Data Analysis. For fluorescence data acquisition and correction of the emission spectra, we used Felix 3.2 software from PTI. All calculations, manipulation, and correction of experimental data were performed in Windows Excel 2000 (Microsoft). Plotting and multiple nonlinear curve fitting (either single or global) were performed using Origin 7.0 (Microcal Software Inc., Northampton, MA).

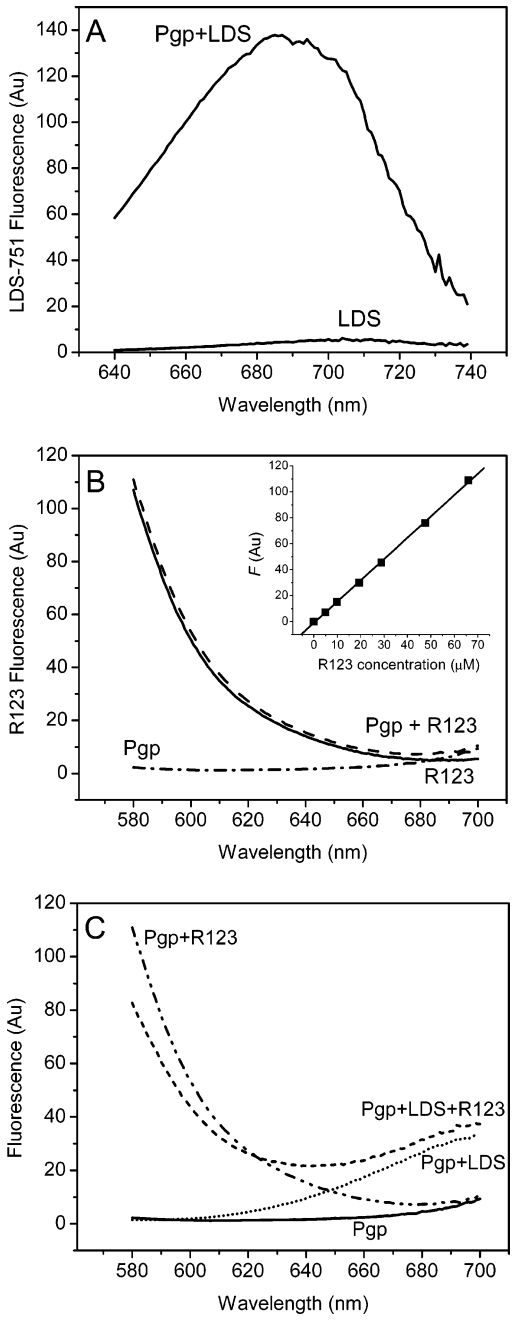

FIGURE 1: (A) Fluorescence emission spectrum of 0.2 μM LDS-751 in 2 mM CHAPS/Tris buffer, and in the same buffer in the presence of 250 μg/mL Pgp. In both cases, the signal from the buffer was subtracted as a blank. The emission bandwidth was 2 nm. (B) Fluorescence emission in the range 580−700 nm of 100 μg/mL Pgp in 2 mM CHAPS/Tris buffer (dashed−dotted line), 5 μM R123 in 2 mM CHAPS/Tris buffer (solid line), and 5 μM R123 with Pgp (100 μg/mL) in 2 mM CHAPS/Tris buffer (dashed line). Inset: corrected fluorescence of R123 in 2 mM CHAPS/Tris buffer. Emission was at 660 nm (4 nm bandwidth). (C) Fluorescence emission spectra for all the Pgp species considered: 100 μg/mL Pgp in 2 mM CHAPS/Tris buffer (solid line), supplemented with 5 μM R123 (dashed−dotted line), with 0.1 μM LDS-751 (dotted line), and with both dyes (dashed line). The emission bandwidth was 4 nm. For all plots, excitation was at 550 nm (4 nm bandwidth), T = 22 °C.

RESULTS

Fluorescent Properties of LDS-751 and R123. Figure 1A shows the emission spectra of LDS-751 in the free and Pgp-bound forms. This dye was previously reported to exhibit an enhancement of fluorescence and blue shift when bound

to Pgp in comparison with aqueous buffer; the changes observed were proposed to be due to the hydrophobic character of the putative binding site for this dye (*35*). This property has been used, among others, to characterize the binding of the dye to the protein. In contrast, the dye R123, which displayed an emission maximum at 530 nm, showed no change in its quantum yield upon binding to the protein (Figure 1B), and made only a slight contribution to the fluorescence at the emission band of LDS-751. The R123 fluorescence should thus show a linear relationship with R123 concentration, regardless of the presence or absence of the protein. Figure 1B (inset) shows that the fluorescence emission intensity at 660 nm and the R123 concentration presented a linear dependence in 2 mM CHAPS/Tris buffer, with $R^2 = 0.99$ in the range tested following excitation at 550 nm. The slope of this line (a proportional factor between fluorescence intensity and R123 concentration in μM^{-1}) is exactly the same in the presence of Pgp (see filled squares in Figures 4A and 4B). The emission spectra of Pgp alone and in the presence of one or both drugs are shown in Figure 1C.

Single Titration of Pgp with LDS-751 in the Presence of R123. By taking advantage of the spectroscopic properties of both dyes, it is possible to study the properties of the binding of LDS-751 to Pgp in the absence and presence of R123, and therefore the interactions between them, by means of fluorescent titration experiments. Following this approach, Figure 2 shows the corrected fluorescence signal from the titration of Pgp with the ligand LDS-751 in the presence of different concentrations of R123. As can be observed, in the absence of Pgp (buffer alone), the corrected signal is linear in the range tested. The linear fitting of this curve led to the molar fluorescence of free LDS-751 at 660 nm, $Q_D = 20.283$ μM^{-1} ($R^2 = 0.985$). The presence of Pgp produces hyperbolic concentration-dependent saturable curves, characteristic of the binding to a single-site model ($n = 1$). The experimental data (5 sets of 13 points each) were fitted by means of a global multiple nonlinear routine to the equation

$$F = F_0 + Q_D[\mathrm{LDS}] + \frac{F_M[\mathrm{LDS}]}{{}^{app}K_d^{LDS} + [\mathrm{LDS}]} \qquad (3)$$

where the total fluorescence F includes the signal from R123, F_0, the linear contribution of free LDS-751, and the saturable contribution of the bound form of the dye.

For this fitting, the parameter Q_D was fixed at the value previously obtained. The maximum value of fluorescence at high concentrations of LDS-751, F_M, was considered a free-floating but *shared* parameter, and was, therefore, constant for the all conditions tested (different R123 concentrations). On the other hand, the apparent dissociation constant for LDS-751, ${}^{app}K_d^{LDS}$, was considered a free-floating but *individual* parameter; that is to say, different for each R123 concentration. The searching algorithm minimized the global quadratic difference, χ^2, reporting the best estimate of the free-floating parameters (Table 1). Setting the parameters, F_M, as *individual* did not improve the fitting, but increased the uncertainty of the estimates. Similarly, setting ${}^{app}K_d^{LDS}$ as *shared* (with the F_M values as *individual*) led to an inappropriate fitting.

As can be seen from Table 1, in the presence of R123, the apparent binding affinity for LDS-751 (as measured by the dissociation constant, K_d) decreased as the R123 concentration increased. A linear relationship between ${}^{app}K_d$ and competitor concentration is expected according to a direct competition model, as indicated by the equation

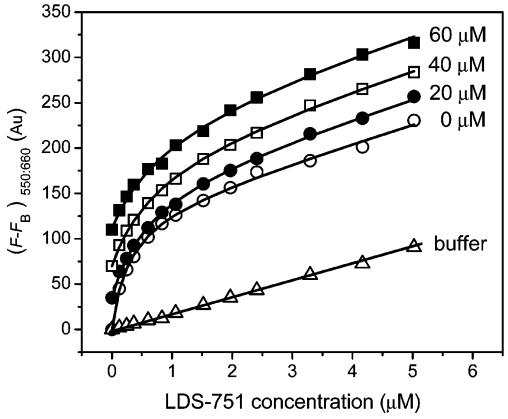

FIGURE 2: Corrected fluorescence ($F - F_B$) of LDS-751 in 2 mM CHAPS/Tris buffer (△), and in 100 μg/mL Pgp in 2 mM CHAPS/Tris buffer with the indicated concentrations of R123. The solid lines represent the best fit to eq 3, setting $F_M = 0$ for the buffer (see text for details). Excitation was at 550 nm, emission at 660 nm (4 nm bandwidth), $T = 22$ °C.

Table 1: Parameters Estimated from the Fitting of Eq 3 to the Data in Figure 2

parameter	estimated value
Q_D (μM^{-1})	20.32 ± 0.15
F_M (au)	130.8 ± 1.1
R123 concn (μM)	**${}^{app}K_d^{LDS}$ (μM)**
0	0.268 ± 0.013
20	0.568 ± 0.025
40	0.760 ± 0.030
60	0.893 ± 0.035

$$ {}^{app}K_d^{LDS} = K_d^{LDS}\left(1 + \frac{[\mathrm{R123}]}{K_d^{R123}}\right) \qquad (4)$$

where K_d^{LDS} and K_d^{R123} are the *true* dissociation constants for LDS-751 and R123, respectively. However, a nonlinear dependence was found, as depicted in Figure 3, suggesting that the interaction between LDS-751 and R123 is noncompetitive. Clearly, this kind of interaction requires that R123 is bound to the protein simultaneously with LDS-751. If this is the case, then each substrate would occupy its own binding site, resulting in the formation of a ternary complex (R123·Pgp·LDS), as shown in Scheme 1.

This type of reaction can be classified as *random binding of two substrates;* binding of the two substrates can be independent or dependent, contingent on whether the interaction factor, w, has a value of unity or not. In this case, the two substrates would interact with each other, reciprocally affecting (reducing) their *true* affinities by a constant factor w. For this binding system, the measured fluorescence at 660 nm can be defined by the equation

$$F = F_0 + Q_D[\mathrm{LDS}] + F_M\left[\frac{\left(\frac{[\mathrm{LDS}]}{K_d^{LDS}}\right) + \left(\frac{[\mathrm{LDS}][\mathrm{R123}]}{wK_d^{LDS}K_d^{R123}}\right)}{1 + \left(\frac{[\mathrm{LDS}]}{K_d^{LDS}}\right) + \left(\frac{[\mathrm{R123}]}{K_d^{R123}}\right) + \left(\frac{[\mathrm{LDS}][\mathrm{R123}]}{wK_d^{LDS}K_d^{R123}}\right)}\right] \qquad (5)$$

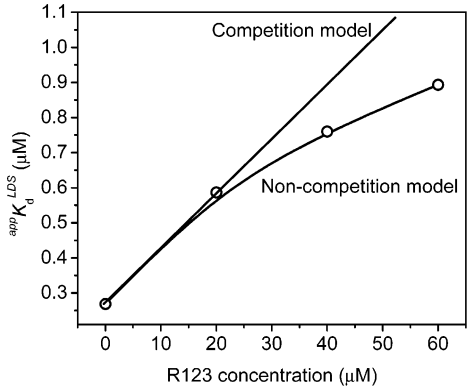

FIGURE 3: Apparent dissociation constant for LDS-751 binding to Pgp, $^{app}K_d^{LDS}$, as a function of the R123 concentration. The linear solid line corresponds to the dependence between both variables using a competition model assumption, simulated according to eq 4. The points represent the values of the parameters shown in Table 1. The curved solid line corresponds to the fitting to eq 6 according to a noncompetition model, with the parameters reported in Table 3.

Scheme 1: Proposed Random Binding Reactions of Pgp (E) with LDS-751 (LDS) and R123[a]

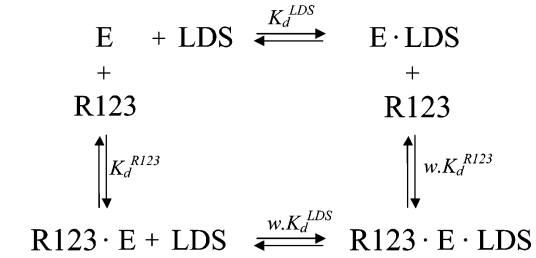

[a] The reaction is characterized by the dissociation constant for LDS-751 (K_d^{LDS}) and for R123 (K_d^{R123}) and by the positive interaction factor (w). E·LDS and R123·E represent the binary complexes between Pgp and LDS-751 and R123, respectively. The position of the substrate before or after E in the complex makes allusion to different binding sites. The ternary complex is depicted as R123·E·LDS.

In this case, the contribution of the bound form of LDS-751 comes from both the binary complex, Pgp·LDS (the first term of the numerator), and the ternary complex, R123·Pgp·LDS (the last term of the numerator). Both bound forms of LDS-751 are grouped under the factor F_M (a parameter that includes, among other things, the total protein concentration and the molar fluorescence of bound LDS-751), assuming that the quantum yield of LDS-751 is unaffected by the binding of R123. That this is indeed the case was suggested by the invariance of this parameter with increasing R123 concentration (see Table 1). In other words, we suggest that the presence of R123 affects the binding properties of LDS-751, but not its fluorescent characteristics, and by extension, its local microenvironment.

It is readily observable that, when either [R123] = 0 or $K_d^{R123} \gg 1$, eq 5 is reduced to eq 3. At any concentration, the extent of occupancy of each binding site is defined by the reduced concentration of the two compounds, ([substrate]/K_d). This variable determines, for a given interaction factor, the magnitude of the influence of one substrate on the apparent affinity of the other. Using eq 5 in a global multiple nonlinear fitting of the 5 sets of experimental data, sharing the parameters F_M but keeping them fixed to the values previously obtained, and allowing the parameters Q_D, w, K_d^{LDS}, and K_d^{R123} to float freely, we estimated the values reported in Table 2.

Table 2: Parameters Estimated from the Fitting of Eq 5 to the Data in Figure 2

parameter	estimated value
Q_D (μM^{-1})	20.28 ± 0.21
F_M (au)	130.8
w	5.45 ± 0.78
K_d^{LDS} (μM)	0.268 ± 0.01
K_d^{R123} (μM)	10.31 ± 1.8

Table 3: Parameters Estimated from the Fitting of Eq 6 to the Data in Figure 3

parameter	estimated value
w	5.52 ± 0.22
K_d^{LDS} (μM)	0.269 ± 0.01
K_d^{R123} (μM)	10.52 ± 0.49

A value of approximately 5.5 was estimated for the interaction factor (Table 2). A value >1 implies that the interaction is negative; in other words, the presence of R123 decreases the affinity of the LDS-751 by over 5-fold, and vice versa. The estimated value for the dissociation constant for R123 obtained here (K_d^{R123}= 10.3 μM) is comparable to the previously published value of 12.8 μM obtained by quenching of 2-(4-maleimidoanilino)naphthalene-6-sulfonic acid (MIANS)-labeled Pgp (*22*). Use of a Trp quenching approach produced a biphasic binding curve (*32*), with K_{d1} = 1.88 and K_{d2} = 29.3 μM (which averages to 15.5 μM), possibly as a result of incomplete corrections of the inner filter effect. The remarkable similarity in the values estimated for the common parameters (Q_D and K_d^{LDS}) using both fitting methods suggests that the proposed model is consistent with the data obtained. Moreover, for this model of substrate interaction, the apparent dissociation constant for LDS-751 would depend on the R123 concentration according to the expression

$$^{app}K_d^{LDS} = K_d^{LDS} + \frac{\left(1 + \frac{[R123]}{K_d^{R123}}\right)}{\left(1 + \frac{[R123]}{wK_d^{R123}}\right)} \qquad (6)$$

By fitting eq 6 using a single nonlinear routine, using the apparent K_d values for LDS-751 at various R123 concentrations (reported in Table 1), it was possible to estimate the parameters w, K_d^{LDS}, and K_d^{R123}. The estimated values obtained are shown in Table 3, and the fitting is depicted in the curve shown in Figure 3. Here again, the relative magnitude of the uncertainties for each parameter, and the similarity of the values obtained using both methods, give an indirect indication of the goodness of the fit and the reliability of the model.

Double Titration of Pgp with LDS-751 and R123. As an alternative fluorescence approach, two double titration experiments were carried out, titrating Pgp first with LDS-751 and then with R123, followed by a separate titration in the reverse order. Figure 4 shows the total corrected fluorescence arising from the titration with LDS-751 (circles)

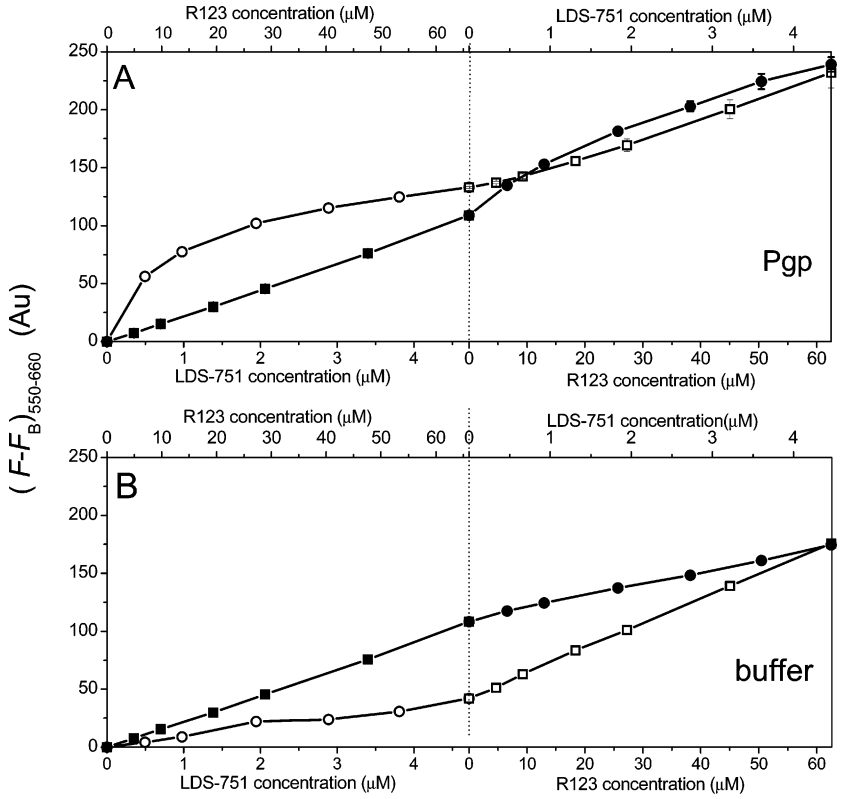

FIGURE 4: Corrected fluorescence at 660 nm (4 nm bandwidth) recorded during titration of (A) 100 μg/mL of Pgp in 2 mM CHAPS/Tris buffer and (B) 2 mM CHAPS/Tris buffer, with LDS-751 (circles) and R123 (squares) in the order LDS-751 first, then R123 (open symbols, bottom *x*-axis) or vice versa (filled symbols, upper *x*-axis). The points represent the average of two determinations ± SD. Where error bars are not visible, they are contained within the symbols. Excitation was at 550 nm (4 nm bandwidth), $T = 22$ °C.

Table 4: Parameters Estimated from the Fitting of Eq 5 to the Data in Figure 5

parameter	estimated value
w	4.91 ± 2.57
K_d^{LDS} (μM)	0.466 ± 0.17
K_d^{R123} (μM)	9.001 ± 1.09

either before or after titration with R123 (squares). The concordance of the final point for titrations carried out in either sequence is remarkable, and effectively indicates that the order of addition of the substrate is random; that is to say, regardless of the order of addition of LDS-751 and R123, the final condition of the system is the same.

For the analysis of these experiments, the data were tabulated according to the three parameters $[LDS]_i$, $[R123]_i$, and F_i^{cor} for both titrations. Fitting both sets of data simultaneously (13 points each) by means of a multivariate multiple routine to eq 5, setting the parameters w, K_d^{LDS}, K_d^{R123} as free-floating, led to the estimates shown in Table 4 and the curves plotted in Figure 5. These values are in reasonable concordance with those obtained earlier using the set of single titrations, although the variation observed for each parameter is higher.

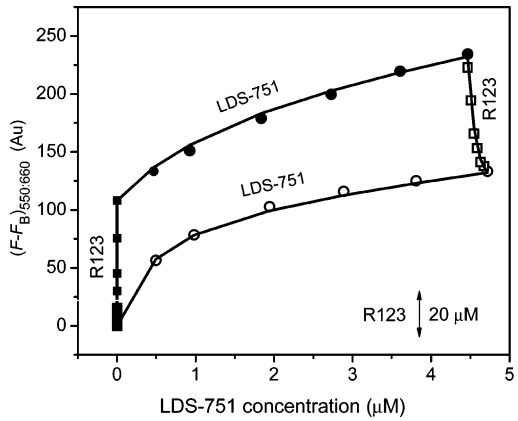

FIGURE 5: The double titration experiments shown in Figure 4A displayed in a single *x*-axis representation. The corrected fluorescence at 660 nm (*y*-axis) is shown, in this case, as a function of the LDS-751 concentration (*x*-axis) and the R123 concentration (inset scale). Symbols are the same as in Figure 4. The solid lines represent the best fit to eq 5 (see text for details).

DISCUSSION

As early as 1989, it was shown that there are at least two photoaffinity labeling sites on Pgp, one in each of the two homologous halves (*41*). More recently, Shapiro and Ling used transport experiments to establish the presence of two "functional" drug-binding sites, referred to as the H-site (preference for H33342 and colchicine) and the R-site (preference for R123 and anthracyclines) (*18*). In this model, the two sites exhibit positive allosteric interactions; R-site substrates stimulate transport of H-site substrates, and vice versa. This simplified two-site model is compatible with competitive and noncompetitive interactions between substrates, as well as cooperativity. In support of this, Wang et al. (*11*) showed that there are at least two binding sites within Pgp, one clearly favoring binding of H33342 and exhibiting noncompetitive interactions with other substrates. Shapiro and Ling established that LDS-751 interacts preferentially with the R-site on Pgp, since sub-micromolar concentrations

of LDS-751 inhibited R123 transport while stimulating transport of H33342. We observed monophasic fluorescence titration curves for both R123 and H33342 (*22*, *42*), suggestive of a single binding site for each drug. We recently showed unambiguously, at the molecular level, that LDS-751 binds directly to Pgp with a sub-micromolar dissociation constant, and the observed monophasic titration curve suggested that the dye also interacts with Pgp via a single site. Using a FRET approach, we mapped the location of the putative R-site to 18−25 Å away from the "line" connecting Cys428 and Cys1071 in the nucleotide-binding (NB) domains (*35*), in accordance with the original suggestion that both the R- and H-sites are probably in the cytoplasmic leaflet of the membrane (*19*, *43*).

In this work, we used fluorescence spectroscopy to study directly the binding equilibrium and relationship between LDS-751 and R123, using purified Pgp. Two different experimental approaches fitted well to a model in which both compounds bind simultaneously and randomly to the protein (Scheme 1). The values obtained for the intrinsic dissociation constants of both dyes (K_d^{LDS} and K_d^{R123}) are close to those previously reported, either by transport experiments (*18*, *19*) or fluorescence approaches (*22*, *35*, *42*), i.e., submicromolar for LDS-751 and 10−12 μM for R123. The transport data obtained for LDS-751 and R123 (*19*) indicated that the drugs interfered with each other, so it was proposed that both were competing for the same site. However, the fluorimetric titrations presented in this work show that, in contrast to the expected mutual exclusion, both of these R-site dyes are capable of coexisting bound to Pgp. In this regard, it is well-known that the functional relationship of competition between two substrates is not conclusive in terms of their structural relationship (i.e., the physical location of the binding sites). A competitive interaction between two substrates does not allow us to distinguish between the possibilities of either a unique shared binding site or two mutually exclusive, but distinct, binding sites, which might be distant sites linked allosterically, or overlapping sites related by steric constraints (see below for further discussion). The coexistence of both bound substrates is not incompatible with the reciprocal inhibition of transport between these dyes reported by Shapiro and Ling (*19*). As they noted, the H- and R-site proposal is a "working model"; it was the simplest interpretation of the results at the time. A nonmutual exclusion between these substrates would also explain the results; the substrates would have individual binding sites, but with a negative reciprocal interaction in the rates of transport ($\beta_i < 1$) and/or their affinities ($\alpha > 1$) (see Scheme 2). We now assess the implications of simultaneous binding of the two substrates to the R-site.

Drug Interactions: Implication for the Binding Affinities. The way in which the binding affinities of the two drugs are modulated shows the linkage between the substrate binding sites. Effectively, LDS-751 and R123 showed a reciprocal negative interaction of approximately 5-fold with respect to their dissociation constants. Negative interaction effects between Pgp substrates were demonstrated as early as 1991, when Tamai and Safa showed "noncompetitive" binding by means of photoaffinity labeling assays (*27*). The magnitude of the effect of the negative heterotropic regulation between drugs and modulators with respect to their dissociation constants has also been reported; for example, (i) several dihydropyridines (nicardipines, nifedipine, and dexniguldipine, among others) accelerate the dissociation of vinblastine from Pgp more than 4-fold (*29*); (ii) SR33557 and verapamil increased the dissociation rate of vinblastine from Pgp by 3- to 4-fold (*30*); (iii) when two different dihydropyridine-binding sites are occupied, they interact with each other to decrease their respective affinities; destabilization factors of 2, 6 and 8 have been reported for nicardipine on binding of nifedipine, nitrendipine, and nimodipine, respectively (*8*); and (iv) two-component quenching curves are observed for binding of many drugs to reconstituted Pgp (*32*, *44*), although is not clear whether they are independent binding sites with intrinsic different affinities or if there is a negative homotropic interaction between them.

Scheme 2: A Compact Reaction Scheme for Energized Pgp (E) Catalyzing the Transport of Two Substrates (S_1 and S_2)[a]

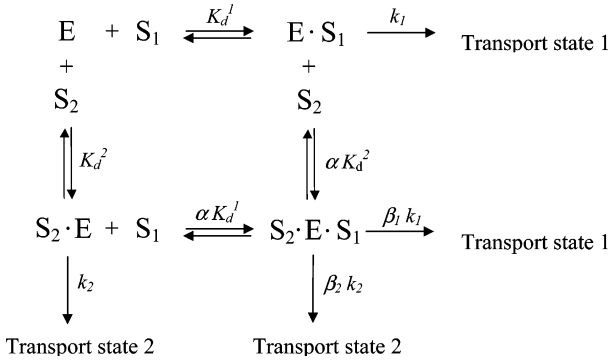

[a] The binary intermediates ($E{\cdot}S_1$ and $E{\cdot}S_2$) are formed according to their respective dissociation constants (K_d^1 and K_d^2), and form the transition states (transport states 1 and 2, respectively) by means of the rate constants k_1 and k_2, respectively. The ternary complex ($S_2{\cdot}E{\cdot}S_1$) can be formed by a random order of binding, and its formation is dictated by the respective dissociation constants and the interaction factor α. In this simplified model, β_1 and β_2 represent the individual factors for the change in rate constant for each substrate, due to the presence of the other substrate in the complex.

Drug Interactions: Implications for Transport. This work shows that LDS-751 and R123 can coexist bound to Pgp. On the other hand, negative interactions in the transport of these substrates were reported (*19*), although the reciprocal inhibition of transport has not yet been characterized rigorously. However, having described the properties of the binding system, we are able to make some precise deductions about the transport system, as follows: (i) Obviously *pure competitive inhibition* (in kinetic terms, $\alpha = \infty$), as suggested by Shapiro and Ling (*19*), is ruled out, since both bound substrates can coexist. (ii) *Pure* noncompetitive inhibition ($\alpha = 1$; $\beta_i = 0$) is also ruled out, since the binding of LDS-751 and R123 was shown not to be independent. We can also rule out *mixed-type inhibition* where affinities either remain constant or are increased ($\alpha \leq 1$; $0 < \beta_i < 1$). Hence, the transport system can be any other that exhibits reduced affinities ($\alpha > 1$), either (iii) *partial competitive inhibition* ($\alpha > 1$; $\beta_i = 1$), where the affinity, but not the rate of transport, is reduced; (iv) *mixed-type inhibition* ($\alpha > 1$; $\beta_i < 1$), where the transport rate is reduced for the ternary complex; or (v) *mixed-type inhibition* ($\alpha > 1$; $\beta_i = 0$), with transport precluded for the ternary complex (for a comprehensive treatment of these models, see ref *45*). The transport factors can be equal or different for each substrate, so that

the system could be, for example, type iv for LDS-751 but type iii for R123, or any other combination among types iii, iv, and v.

There are plentiful data in the literature indicating noncompetitive and mixed-type inhibition between substrate and modulators, revealed by transport and kinetic measurements (*7*, *8*, *10*, *11*, *13*, *14*, *46*−*48*), but no clear consensus on the number and relationships of the drug and modulator binding sites has yet emerged. Obviously for a two-substrate assay, data analysis is more straightforward for a binding system than for a transport system. The situation is even more complex in the case of ATPase activity, where the real substrate is the ATP, while drugs are ligands that modulate this activity. This has been part of the confusion and misunderstanding with respect to the number, location, and relationships of the drug and modulator binding sites reported in the literature. For example, sometimes transport or enzymatic reactions (drug transport or ATP hydrolysis) have been treated as binding experiments, steady-state data for radioligand transport have been treated as initial rate data, photoaffinity labeling sites have been considered as binding sites, kinetic relationships have been misinterpreted as structural relationships, and so on. However, some approaches have been rigorous. For example, Wang et al. (*11*) correctly employed analysis of Pgp-ATPase activity to study the interaction of H33342 with other ligands: (i) in the case of tetraphenylphosphonium (TPP^+), the estimated affinity perturbation factor was ~4-fold and reciprocal inhibition resulted in a mixed-type pattern of inhibition with a ternary complex whose activity was about one-third of the maximum; (ii) in the case of verapamil, the affinity perturbation factor was ~2- to 3-fold and the ternary complex seemed to exhibit no activity.

Drug Interactions: Models. The original two-site model of Shapiro and Ling must be updated with new experimental evidence. The same authors already suggested the existence of a third drug-binding site on Pgp (the P-site) with a positive allosteric effect on drug transport by the H- and R-sites (*20*). Recently, Wang et al. (*49*) studied the effect of several green tea catechins on LDS-751 and R123 transport in whole cells, finding that a particular catechin stimulated LDS-751 transport and inhibited R123 transport (and vice versa). This observation represents additional evidence that LDS-751 and R123 bind to distinct "physical" sites, since it is hard to imagine that a particular catechin would be able to differentially modulate the transport of two different compounds that interact with the same site. In this regard, the multisite model proposed by Pascaud et al. (*8*) considers that Pgp has different binding sites for drugs and modulators, which exhibit all possible relationships: mutual exclusion ($\alpha = \infty$), mutual interaction ($\alpha \neq 1$), or complete independence ($\alpha = 1$). Furthermore, Martin and co-workers (*50*) detected at least four distinct binding sites exhibiting mutual allosteric interactions, and Wang et al. (*11*) reported Hill coefficients ranging from 1 to 5 for inhibition of daunorubicin transport by several ligands.

Drug Interactions: Structural Implications. One explanation for the negative binding interaction between LDS-751 and R123 is allosteric dependence between different, distant binding sites, where conformational changes are a prerequisite for substrates to interact allosterically. Few studies on conformational changes following substrate binding to Pgp have been carried out so far, and they have focused mainly on the interaction between the drug binding sites and NB domains, or on changes taking place during the catalytic cycle (*31*, *32*, *51*−*55*). Sonveaux et al. did not find significant alterations in the secondary structure of Pgp following verapamil binding (*56*), while Liu et al. (*32*), contrary to a previous report (*56*), found changes in Trp susceptibility to acrylamide quenching following binding of three different substrates. An indirect indicator of "interaction at a distance" is shown by the positive interactions between ligands; cooperativity of binding, either heterotropic or homotropic, is strong evidence for allosteric interaction. Stimulatory effects of one ligand on binding of another have emerged from photoaffinity labeling studies (for example, see refs *57*, *58*) or transport experiments (*18*, *49*). In addition, two groups showed an increase in the rate of dissociation of one drug from Pgp by interaction with another (*29*, *30*, *50*), which can only be explained by allosteric modulation.

An alternate explanation for a negative binding interaction between two substrates is that the sites are adjacent, very close, and overlapping. The two sites are intrinsically independent, but with steric constraints; binding of the first drug molecule partially blocks binding of the second via steric hindrance, thus reducing its effective binding affinity. It can be proposed that TM helices from both halves of Pgp form a single drug-binding region with distinct but overlapping specificities, which would explain the broad substrate tolerance of the transporter. A large, common hydrophobic pocket, which can accommodate different substrates using a combination of residues from different TMs, could form a binding site for a particular drug according to the substrate-induced fit hypothesis (*59*). Aromatic side chains, such as Trp residues, in the TM segments may play a central role in substrate binding (*60*), explaining the high level of Trp quenching on binding of certain drugs (*32*). Studies by Clarke and co-workers using Cys mutants and thiol-reactive substrate analogues support the idea of a common hydrophobic pocket, and show that residues from multiple TM segments contribute to the binding region (*5*, *61*−*63*). Additionally, the dimensions of the pocket, determined using a thiol-reactive cross-linking substrate, indicate that it may accommodate more than one substrate at the same time (*64*). Using the thiol-reactive substrate tris(2-maleimidoethyl)amine (TMEA) and a second drug, they recently showed that TMEA-mediated cross-linking of neighboring Cys residues in Pgp mutants was stimulated by verapamil but not by colchicine, rhodamine B, and several other drugs (*65*), thus suggesting that TMEA and another drug molecule can simultaneously occupy different regions of the binding pocket. It is clear that, with the binding data obtained in the present work, a firm conclusion about the location of the binding sites for LDS-751 and R123, and their structural relationship, is not possible. However, it seems clear that the putative R-site, if it exists physically, is a large pocket flexible enough to accommodate both substrates by means of overlapping regions. On the other hand, it is possible that it consists of two smaller distant sites, each specific for particular drugs yet allosterically linked, so that the R-site is just a phenomenological description of the effect of compounds that bind to it on the transport of H-site substrates.

The complex binding modes of multiple drugs have been elucidated for the soluble multidrug-binding transcription repressors QacR (from *S. aureus*) (*66*) and BmrR (from *B. subtilis*) (*67*) using X-ray crystallography of the proteins complexed with several different compounds. Each drug was observed to interact with the protein using a different binding mode, although some drugs shared a similar physical space in a "minipocket" inside the large binding cavity. Structural studies on the proton antiporter multidrug efflux pump AcrB from *Escherichia coli* (a member of the MF superfamily) complexed with four different ligands came to similar conclusions (*68*). Three drug molecules were observed to bind simultaneously to the transporter using a different subset of AcrB residues. Simultaneous binding of two drugs to QacR was shown recently by Brennan and co-workers (*69*). X-ray crystal structures showed that Rhodamine 6G and proflavin interact with QacR using the same minipocket, where they interfere sterically with each other, making simultaneous binding of both drugs impossible. In contrast, ethidium and proflavin bind to different, but partially overlapping minipockets, so that both drugs can bind at the same time. Similar principles may apply to Pgp, but detailed structural information on the Pgp molecule complexed to various substrates will be needed before details such this can be addressed.

REFERENCES

1. Goldie, J. H. (2001) Drug resistance in cancer: A perspective, *Cancer Metastasis Rev. 20*, 63−68.
2. Gottesman, M. M., Fojo, T., and Bates, S. E. (2002) Multidrug resistance in cancer: role of ATP-dependent transporters, *Nat. Rev. Cancer 2*, 48−58.
3. Schinkel, A. H., and Jonker, J. W. (2003) Mammalian drug efflux transporters of the ATP binding cassette (ABC) family: an overview, *Adv. Drug Delivery Rev. 55*, 3−29.
4. Kim, R. B. (2002) Drugs as P-glycoprotein substrates, inhibitors, and inducers, *Drug Metab. Rev. 34*, 47−54.
5. Loo, T. W., and Clarke, D. M. (1999) Identification of residues in the drug-binding domain of human P-glycoprotein−Analysis of transmembrane segment 11 by cysteine-scanning mutagenesis and inhibition by dibromobimane, *J. Biol. Chem. 274*, 35388−35392.
6. Sharom, F. J., Yu, X., Chu, J. W. K., and Doige, C. A. (1995) Characterization of the ATPase activity of P-glycoprotein from multidrug-resistant Chinese hamster ovary cells, *Biochem. J. 308*, 381−390.
7. Litman, T., Zeuthen, T., Skovsgaard, T., and Stein, W. D. (1997) Competitive, non-competitive and cooperative interactions between substrates of P-glycoprotein as measured by its ATPase activity, *Biochim. Biophys. Acta 1361*, 169−176.
8. Pascaud, C., Garrigos, M., and Orlowski, S. (1998) Multidrug resistance transporter P-glycoprotein has distinct but interacting binding sites for cytotoxic drugs and reversing agents, *Biochem. J. 333*, 351−358.
9. Borgnia, M. J., Eytan, G. D., and Assaraf, Y. G. (1996) Competition of hydrophobic peptides, cytotoxic drugs, and chemosensitizers on a common P-glycoprotein pharmacophore as revealed by its ATPase activity, *J. Biol. Chem. 271*, 3163−3171.
10. Orlowski, S., Mir, L. M., Belehradek, J. J., and Garrigos, M. (1996) Effects of steroids and verapamil on P-glycoprotein ATPase activity: progesterone, desoxycorticosterone, corticosterone and verapamil are mutually non-exclusive modulators, *Biochem. J. 317*, 515−522.
11. Wang, E. J., Casciano, C. N., Clement, R. P., and Johnson, W. W. (2000) Two transport binding sites of P-glycoprotein are unequal yet contingent: initial rate kinetic analysis by ATP hydrolysis demonstrates intersite dependence, *Biochim. Biophys. Acta 1481*, 63−74.
12. DiDiodato, G., and Sharom, F. J. (1997) Interaction of combinations of drugs, chemosensitizers, and peptides with the P-glycoprotein multidrug transporter, *Biochem. Pharmacol. 53*, 1789−1797.
13. Ayesh, S., Shao, Y. M., and Stein, W. D. (1996) Co-operative, competitive and non-competitive interactions between modulators of P-glycoprotein, *Biochim. Biophys. Acta 1316*, 8−18.
14. Shao, Y. M., Ayesh, S., and Stein, W. D. (1997) Mutually co-operative interactions between modulators of P-glycoprotein, *Biochim. Biophys. Acta 1360*, 30−38.
15. Essodaigui, M., Broxterman, H. J., and Garnier-Suillerot, A. (1998) Kinetic analysis of calcein and calcein-acetoxymethylester efflux mediated by the multidrug resistance protein and P-glycoprotein, *Biochemistry 37*, 2243−2250.
16. Loetchutinat, C., Saengkhae, C., Marbeuf-Gueye, C., and Garnier-Suillerot, A. (2003) New insights into the P-glycoprotein-mediated effluxes of rhodamines, *Eur. J. Biochem. 270*, 476−485.
17. Shapiro, A. B., Corder, A. B., and Ling, V. (1997) P-glycoprotein-mediated Hoechst 33342 transport out of the lipid bilayer, *Eur. J. Biochem. 250*, 115−121.
18. Shapiro, A. B., and Ling, V. (1997) Positively cooperative sites for drug transport by P-glycoprotein with distinct drug specificities, *Eur. J. Biochem. 250*, 130−137.
19. Shapiro, A. B., and Ling, V. (1998) Transport of LDS-751 from the cytoplasmic leaflet of the plasma membrane by the rhodamine-123-selective site of P-glycoprotein, *Eur. J. Biochem. 254*, 181−188.
20. Shapiro, A. B., Fox, K., Lam, P., and Ling, V. (1999) Stimulation of P-glycoprotein-mediated drug transport by prazosin and progesterone. Evidence for a third drug-binding site, *Eur. J. Biochem. 259*, 841−850.
21. Shapiro, A. B., and Ling, V. (1995) Reconstitution of drug transport by purified P-glycoprotein, *J. Biol.* Chem. *270*, 16167−16175.
22. Lu, P., Liu, R., and Sharom, F. J. (2001) Drug transport by reconstituted P-glycoprotein in proteoliposomes−Effect of substrates and modulators, and dependence on bilayer phase state, *Eur. J. Biochem. 268*, 1687−1697.
23. Morris, D. I., Greenberger, L. M., Bruggemann, E. P., Cardarelli, C., Gottesman, M. M., Pastan, I., and Seamon, K. B. (1994) Localization of the forskolin labeling sites to both halves of P-glycoprotein: similarity of the sites labeled by forskolin and prazosin, *Mol. Pharmacol. 46*, 329−337.
24. Isenberg, B., Thole, H., Tümmler, B., and Demmer, A. (2001) Identification and localization of three photobinding sites of iodoarylazidoprazosin in hamster P-glycoprotein, *Eur. J. Biochem. 268*, 2629−2634.
25. Borchers, C., Ulrich, W. R., Klemm, K., Ise, W., Gekeler, V., Haas, S., Schodl, A., Conrad, J., Przybylski, M., and Boer, R. (1995) B9209-005, an azido derivative of the chemosensitizer dexniguldipine-HCl, photolabels P-glycoprotein, *Mol. Pharmacol. 48*, 21−29.
26. Pleban, K., Kopp, S., Csaszar, E., Peer, M., Hrebicek, T., Rizzi, A., Ecker, G. F., and Chiba, P. (2005) P-glycoprotein substrate binding domains are located at the transmembrane domain/transmembrane domain interfaces: A combined photoaffinity labeling-protein homology modeling approach, *Mol. Pharmacol. 67*, 365−374.
27. Tamai, I., and Safa, A. R. (1991) Azidopine noncompetitively interacts with vinblastine and cyclosporin A binding to P-glycoprotein in multidrug resistant cells, *J. Biol. Chem. 266*, 16796−16800.
28. Ferry, D. R., Russell, M. A., and Cullen, M. H. (1992) P-glycoprotein possesses a 1,4-dihydropyridine-selective drug acceptor site which is allosterically coupled to a vinca-alkaloid-selective binding site, *Biochem. Biophys. Res. Commun. 188*, 440−445.
29. Ferry, D. R., Malkhandi, P. J., Russell, M. A., and Kerr, D. J. (1995) Allosteric regulation of [3H]vinblastine binding to P-glycoprotein of MCF-7 ADR cells by dexniguldipine, *Biochem. Pharmacol. 49*, 1851−1861.
30. Martin, C., Berridge, G., Higgins, C. F., and Callaghan, R. (1997) The multi-drug resistance reversal agent SR33557 and modulation of vinca alkaloid binding to P-glycoprotein by an allosteric interaction, *Br. J. Pharmacol. 122*, 765−771.
31. Liu, R., and Sharom, F. J. (1996) Site-directed fluorescence labeling of P-glycoprotein on cysteine residues in the nucleotide binding domains, *Biochemistry 35*, 11865−11873.

32. Liu, R., Siemiarczuk, A., and Sharom, F. J. (2000) Intrinsic fluorescence of the P-glycoprotein multidrug transporter: Sensitivity of tryptophan residues to binding of drugs and nucleotides, *Biochemistry 39*, 14927−14938.
33. Sharom, F. J., Liu, R., and Romsicki, Y. (1998) Spectroscopic and biophysical approaches for studying the structure and function of the P-glycoprotein multidrug transporter, *Biochem. Cell Biol. 76*, 695−708.
34. Sharom, F. J., Liu, R., Romsicki, Y., and Lu, P. (1999) Insights into the structure and substrate interactions of the P-glycoprotein multidrug transporter from spectroscopic studies, *Biochim. Biophys. Acta 1461*, 327−345.
35. Lugo, M. R., and Sharom, F. J. (2005) Interaction of LDS-751 with P-glycoprotein and mapping of the location of the R drug binding site, *Biochemistry 44*, 643−655.
36. Doige, C. A., and Sharom, F. J. (1991) Strategies for the purification of P-glycoprotein from multidrug-resistant Chinese hamster ovary cells, *Protein Expression Purif. 2*, 256−265.
37. Peterson, G. L. (1977) A simplification of the protein assay method of Lowry et al. which is more generally applicable, *Anal. Biochem. 83*, 346−356.
38. Bradford, M. M. (1976) A rapid and sensitive method for the quantitation of microgram quantities of protein utilizing the principle of protein-dye binding, *Anal. Biochem. 72*, 248−254.
39. Lakowicz, J. R. (1999) *Principles of Fluorescence Spectroscopy*, Kluwer Academic Publishers, New York.
40. Birdsall, B., King, R. W., Wheeler, M. R., Lewis, C. A., Jr., Goode, S. R., Dunlap, R. B., and Roberts, G. C. (1983) Correction for light absorption in fluorescence studies of protein-ligand interactions, *Anal. Biochem. 132*, 353−361.
41. Bruggemann, E. P., Germann, U. A., Gottesman, M. M., and Pastan, I. (1989) Two different regions of P-glycoprotein are photoaffinity-labeled by azidopine, *J. Biol. Chem. 264*, 15483−15488.
42. Qu, Q., Chu, J. W., and Sharom, F. J. (2003) Transition state P-glycoprotein binds drugs and modulators with unchanged affinity, suggesting a concerted transport mechanism, *Biochemistry 42*, 1345−1353.
43. Shapiro, A. B., and Ling, V. (1997) Extraction of Hoechst 33342 from the cytoplasmic leaflet of the plasma membrane by P-glycoprotein, *Eur. J. Biochem. 250*, 122−129.
44. Romsicki, Y., and Sharom, F. J. (1999) The membrane lipid environment modulates drug interactions with the P-glycoprotein multidrug transporter, *Biochemistry 38*, 6887−6896.
45. Segel, I. H. (1975) *Enzyme Kinetics*, John Wiley and Sons, New York.
46. Spoelstra, E. C., Westerhoff, H. V., Pinedo, H. M., Dekker, H., and Lankelma, J. (1994) The multidrug-resistance-reverser verapamil interferes with cellular P-glycoprotein-mediated pumping of daunorubicin as a non-competing substrate, *Eur. J. Biochem. 221*, 363−373.
47. Pereira, E., Borrel, M. N., Fiallo, M., and Garnier-Suillerot, A. (1994) Non-competitive inhibition of P-glycoprotein-associated efflux of THP-adriamycin by verapamil in living K562 leukemia cells, *Biochim. Biophys. Acta 1225*, 209−216.
48. Garrigos, M., Mir, L. M., and Orlowski, S. (1997) Competitive and non-competitive inhibition of the multidrug-resistance-associated P-glycoprotein ATPase-further experimental evidence for a multisite model, *Eur. J. Biochem. 244*, 664−673.
49. Wang, E. J., Barecki-Roach, M., and Johnson, W. W. (2002) Elevation of P-glycoprotein function by a catechin in green tea, *Biochem. Biophys. Res. Commun. 297*, 412−418.
50. Martin, C., Berridge, G., Higgins, C. F., Mistry, P., Charlton, P., and Callaghan, R. (2000) Communication between multiple drug binding sites on P-glycoprotein, *Mol. Pharmacol. 58*, 624−632.
51. Liu, R., and Sharom, F. J. (1997) Fluorescence studies on the nucleotide binding domains of the P-glycoprotein multidrug transporter, *Biochemistry 36*, 2836−2843.
52. Mechetner, E. B., Schott, B., Morse, B. S., Stein, W. D., Druley, T., Davis, K. A., Tsuruo, T., and Roninson, I. B. (1997) P-glycoprotein function involves conformational transitions detectable by differential immunoreactivity, *Proc. Natl. Acad. Sci. U.S.A. 94*, 12908−12913.
53. Qu, Q., and Sharom, F. J. (2001) FRET analysis indicates that the two ATPase active sites of the P-glycoprotein multidrug transporter are closely associated, *Biochemistry 40*, 1413−1422.
54. Qu, Q., and Sharom, F. J. (2002) Proximity of bound Hoechst 33342 to the ATPase catalytic sites places the drug binding site of P-glycoprotein within the cytoplasmic membrane leaflet, *Biochemistry 41*, 4744−4752.
55. Rosenberg, M. F., Velarde, G., Ford, R. C., Martin, C., Berridge, G., Kerr, I. D., Callaghan, R., Schmidlin, A., Wooding, C., Linton, K. J., and Higgins, C. F. (2001) Repacking of the transmembrane domains of P-glycoprotein during the transport ATPase cycle, *EMBO J. 20*, 5615−5625.
56. Sonveaux, N., Shapiro, A. B., Goormaghtigh, E., Ling, V., and Ruysschaert, J. M. (1996) Secondary and tertiary structure changes of reconstituted P-glycoprotein. A Fourier transform attenuated total reflection infrared spectroscopy analysis, *J. Biol. Chem. 271*, 24617−24624.
57. Safa, A. R., Roberts, S., Agresti, M., and Fine, R. L. (1994) Tamoxifen aziridine, a novel affinity probe for P-glycoprotein in multidrug resistant cells, *Biochem. Biophys. Res. Commun. 202*, 606−612.
58. Dey, S., Ramachandra, M., Pastan, I., Gottesman, M. M., and Ambudkar, S. V. (1997) Evidence for two nonidentical drug-interaction sites in the human P-glycoprotein, *Proc. Natl. Acad. Sci. U.S.A. 94*, 10594−10599.
59. Loo, T. W., Bartlett, M. C., and Clarke, D. M. (2003) Substrate-induced conformational, changes in the transmembrane segments of human P-glycoprotein−Direct evidence for the substrate-induced fit mechanism for drug binding, *J. Biol. Chem. 278*, 13603−13606.
60. Pawagi, A. B., Wang, J., Silverman, M., Reithmeier, R. A., and Deber, C. M. (1994) Transmembrane aromatic amino acid distribution in P-glycoprotein. A functional role in broad substrate specificity, *J. Mol. Biol. 235*, 554−564.
61. Loo, T. W., and Clarke, D. M. (1997) Identification of residues in the drug-binding site of human P-glycoprotein using a thiol-reactive substrate, *J. Biol. Chem. 272*, 31945−31948.
62. Loo, T. W., and Clarke, D. M. (2001) Defining the drug-binding site in the human multidrug resistance P-glycoprotein using a methanethiosulfonate analog of verapamil, MTS-verapamil, *J. Biol. Chem. 276*, 14972−14979.
63. Loo, T. W., and Clarke, D. M. (2002) Location of the rhodamine-binding site in the human multidrug resistance P-glycoprotein, *J. Biol. Chem. 277*, 44332−44338.
64. Loo, T. W., and Clarke, D. M. (2001) Determining the dimensions of the drug-binding domain of human P-glycoprotein using thiol cross-linking compounds as molecular rulers, *J. Biol. Chem. 276*, 36877−36880.
65. Loo, T. W., Bartlett, M. C., and Clarke, D. M. (2003) Simultaneous binding of two different drugs in the binding pocket of the human multidrug resistance P-glycoprotein, *J. Biol. Chem. 278*, 39706−39710.
66. Schumacher, M. A., Miller, M. C., Grkovic, S., Brown, M. H., Skurray, R. A., and Brennan, R. G. (2001) Structural mechanisms of QacR induction and multidrug recognition, *Science 294*, 2158−2163.
67. Zheleznova, E. E., Markham, P. N., Neyfakh, A. A., and Brennan, R. G. (1999) Structural basis of multidrug recognition by BmrR, a transcription activator of a multidrug transporter, *Cell 96*, 353−362.
68. Yu, E. W., McDermott, G., Zgurskaya, H. I., Nikaido, H., and Koshland, D. E., Jr. (2003) Structural basis of multiple drug-binding capacity of the AcrB multidrug efflux pump, *Science 300*, 976−980.
69. Schumacher, M. A., Miller, M. C., and Brennan, R. G. (2004) Structural mechanism of the simultaneous binding of two drugs to a multidrug-binding protein, *EMBO J. 23*, 2923−2930.

BI0511179